Modeling and Quantification of Repolarization Feature Dependency on Heart Rate

A. Minchole[1,2,3]; E. Zacur[3]; E. Pueyo[2,3]; P. Laguna[3,2]

[1]Department of Computer Science, University of Oxford, Oxford, UK;
[2]Biomedical Research Networking Center in Bioengineering, Biomaterials and Nanomedicine (CIBER-BBN), Zaragoza, Spain;
[3]I3A, Universidad de Zaragoza, Zaragoza, Spain

Keywords
Rate adaptation, T-peak to T-end, QT interval

Summary

Introduction: This article is part of the Focus Theme of *Methods of Information in Medicine* on "Biosignal Interpretation: Advanced Methods for Studying Cardiovascular and Respiratory Systems".

Objectives: This work aims at providing an efficient method to estimate the parameters of a non linear model including memory, previously proposed to characterize rate adaptation of repolarization indices.

Methods: The physiological restrictions on the model parameters have been included in the cost function in such a way that unconstrained optimization techniques such as descent optimization methods can be used for parameter estimation. The proposed method has been evaluated on electrocardiogram (ECG) recordings of healthy subjects performing a tilt test, where rate adaptation of QT and Tpeak-to-Tend (T_{pe}) intervals has been characterized.

Results: The proposed strategy results in an efficient methodology to characterize rate adaptation of repolarization features, improving the convergence time with respect to previous strategies. Moreover, T_{pe} interval adapts faster to changes in heart rate than the QT interval.

Conclusions: In this work an efficient estimation of the parameters of a model aimed at characterizing rate adaptation of repolarization features has been proposed. The T_{pe} interval has been shown to be rate related and with a shorter memory lag than the QT interval.

Correspondence to:
Ana Minchole
Department of Computer Science
University of Oxford
Wolfson Building
Parks Road
Oxford, OX1 3QD
United Kingdom
E-mail: ana.minchole@cs.ox.ac.uk

Methods Inf Med 2014; 53: 324–328
doi: 10.3414/ME13-02-0040
received: October 14, 2013
accepted: June 3, 2014
Epub ahead of print: ■■■

1. Introduction

The QT and Tpeak-to-Tend (T_{pe}) intervals are commonly used to describe overall repolarization duration and its spatial dispersion from the electrocardiogram (ECG). Prolongations of these intervals have been related to increased arrhythmic risk under a variety of clinical conditions [1].

The QT interval is known to be influenced by changes in heart rate (HR) and the use of HR correction is crucial in the estimation of QT prolongation. However, the rate dependence of the T_{pe} interval is still an issue. Previous studies characterizing T_{pe} rate dependence are controversial, with T_{pe} shown to be independent of HR by some authors [2] and markedly HR dependent by others [3, 4].

In this work, a model previously proposed to estimate QT rate adaptation [5] was used to estimate both QT and T_{pe} rate adaptations. In [5], the DiRect method, which is a derivative free optimizer, was used to solve the model in the QT case. The physiological restrictions on the model parameters and the computational time required for the estimation led us to propose an efficient estimation method that uses a quasi-Newton optimization technique.

The proposed method was evaluated in ECG recordings presenting changes in the RR interval in which T_{pe} rate adaptation was characterized and compared to QT adaptation.

2. Methods

2.1 Model Formulation

The model illustrated in ▶Figure 1 describes the relationship between the RR interval series (input) and the T_{pe} series $y_{Tpe}[n]$ (output), sampled to 1 Hz. The problem consists in the identification of two blocks, a FIR filter and a nonlinear function, which relate $x_{RR}[n]$ and $y_{Tpe}[n]$ (analogously $x_{RR}[n]$ and $y_{QT}[n]$).

The first block corresponds to a time invariant Nth-order FIR filter with impulse response:

$$\mathbf{h} = (h[1], \ldots, h[N])^T$$

whose output is denoted by $z_{RR}[n]$. The impulse response $\mathbf{h}$ includes information about the memory of the system, that is, a characterization of the influence of pre-

vious RR intervals on each T_{pe} measurement. The order N of the filter was set to 150 samples after sampling to 1 Hz corresponding to 150 seconds, expected to exceed the T_{pe} and QT memory lag for the population used in this study.

The second block is a function $g_k(., \mathbf{a})$, which is parameterized by the vector $\mathbf{a} = [a_0, a_1]^T$. $g_k(., \mathbf{a})$ represents the relationship between the RR interval and the T_{pe} interval once the memory effect has been compensated for, and in this study it was particularized and optimized for each subject using one of the regression functions g_k described below.

The output of the model $\hat{y}_{Tpe}[n]$ is defined as:

$$\hat{y}_{Tpe}[n] = g_k(z_{RR}[n], \mathbf{a}) \quad (1)$$

In vector notation, $\boldsymbol{z}_{RR}$, is the convolution between the input vector $\boldsymbol{x}_{RR}$ and the impulse response $\mathbf{h}$, and can be expressed as $\boldsymbol{z}_{RR} = \boldsymbol{x}_{RR} \cdot \mathbf{h} = \mathbf{X}_{RR}\boldsymbol{h}$, where $\boldsymbol{X}_{RR}$ is the Toeplitz matrix of $\boldsymbol{x}_{RR}$:

$$\boldsymbol{X}_{RR} = \begin{pmatrix} x_{RR}[N] & x_{RR}[N-1] & \dots & x_{RR}[1] \\ x_{RR}[N+1] & x_{RR}[N] & \ddots & \vdots \\ \vdots & \vdots & \ddots & \vdots \\ x_{RR}[M] & x_{RR}[M-1] & \dots & x_{RR}[M-N+1] \end{pmatrix}$$

which is a (M − N + 1) × N matrix, where M is the length of the signal $\boldsymbol{x}_{RR}$.

Different biparametric regression functions that span from a linear to a hyperbolic relationship, as described in [5], were considered for $g_k(\cdot, \mathbf{a})$, and the one that best fitted the data of each subject was identified. Three examples are:

Linear: $$\hat{y}_{Tpe}[n] = g_1(z_{RR}[n], \mathbf{a}) = a_0 + a_1 z_{RR}[n] \quad (2)$$

Hyperbolic: $$\hat{y}_{Tpe}[n] = g_2(z_{RR}[n], \mathbf{a}) = a_0 + \frac{a_1}{z_{RR}[n]} \quad (3)$$

Parabolic: $$\hat{y}_{Tpe}[n] = g_3(z_{RR}[n], \mathbf{a}) = a_0 \cdot z_{RR}[n]^{a_1} \quad (4)$$

The optimum values of the FIR filter response $\mathbf{h}$, function g_k and vector $\mathbf{a}$, were searched for by minimizing a least square estimator between the estimated output $\hat{y}_{Tpe}[n]$ (▶Equation 1) and $y_{Tpe}[n]$, for each subject independently using its whole recording. However, as described in [5], this optimization problem is an "ill-posed" problem, where a regularization term including a priori information of the solution should be added. In this a Tikhonov regularization approach was used [6]. Rate dependence of repolarization features was modeled as an exponential decay. Deviations of $\mathbf{h}$ from having an exponential decay were penalized by considering the following regularization matrix $\boldsymbol{D}$ (5):

$$\boldsymbol{D} = \begin{bmatrix} \tau & -1 & 0 & \dots & 0 \\ 0 & \tau & -1 & \ddots & \vdots \\ \vdots & \ddots & \ddots & \ddots & 0 \\ 0 & \dots & 0 & \tau & -1 \end{bmatrix}$$

Note that in case of $\mathbf{h}$ having an exponential decay expressed as $h[j] = e^{-\lambda j} = \tau^j$, the equality $\|\boldsymbol{D}\mathbf{h}\| = 0$ holds.

The value of τ was estimated as the best exponential decay of $\mathbf{h}$ that leads to the minimum mean square error between $y_{Tpe}[n]$ and $\hat{y}_{Tpe}[n]$ using the linear regression model g_1.

The estimator thus turns into a regularized least square estimator:

$$\{\mathbf{h}^\star, \mathbf{a}^\star, k^\star\} = \arg\min_{\{\mathbf{h}, \mathbf{a}, k\}}(J_k(\mathbf{h}, \mathbf{a})) \quad (5)$$

with $J_k(\mathbf{h}, \mathbf{a})$, the cost function to be minimized for each regression model, defined as:

$$J_k(\mathbf{h}, \mathbf{a}) = \|y_{Tpe} - g_k(\boldsymbol{x}_{RR} \cdot \mathbf{h}, \mathbf{a})\|^2 + \beta^2\|\boldsymbol{D}\mathbf{h}\|^2. \quad (6)$$

In the above expression β^2 is a regularization parameter that controls the weight given to the regularization energy $\|\boldsymbol{D}\mathbf{h}\|^2$ relative to the residual energy $\|y_{Tpe} - \hat{y}_{Tpe}\|^2$. In this study the value of β was obtained by using the "L-curve" criterion [7].

Regarding $k^\star$ in ▶Equation 5, the optimum regression function $g_k(\cdot, \mathbf{a})$ was determined as the one that minimizes the mean square error for each subject independently.

Additionally, in the above described problem, the optimal estimation of $\mathbf{h}$ was subject to two constraints: the sum of the $\mathbf{h}$ components has to be 1 ($\sum_{i=1}^{N} h[i] = 1$) to ensure normalized filter gain, and all the components of $\mathbf{h}$ have to be non-negative ($h[i] \geq 0$) to give a physiological plausible interpretation.

2.2 Optimization Including Restrictions

In this work we reparameterized $J_k(\mathbf{h}, \mathbf{a})$ in order to incorporate the two restrictions and we used a "quasi-Newton" optimization technique to minimize the new cost function.

In order to minimize the cost function in ▶Equation 6, subject to the previously described constraints, we defined $h[j] = \frac{\tilde{h}[j]^2}{\sum_i \tilde{h}[i]^2}$, and optimized over $\tilde{\mathbf{h}}$ without any constraints. The new cost function was:

$$\tilde{J}_k(\tilde{\mathbf{h}}, \mathbf{a}) = J_k\left(\frac{\tilde{\mathbf{h}}^2}{\sum \tilde{h}[i]^2}, \mathbf{a}\right)$$

over which unconstrained optimization techniques can be used. $\tilde{\mathbf{h}}^2$ is defined as $\tilde{\mathbf{h}}^2 = [\tilde{h}[1]^2, \dots, \tilde{h}[N]^2]$. The function $\tilde{J}_k(\tilde{\mathbf{h}}, \mathbf{a})$ was optimized over $\tilde{\mathbf{h}}$ and over $\mathbf{a}$ for

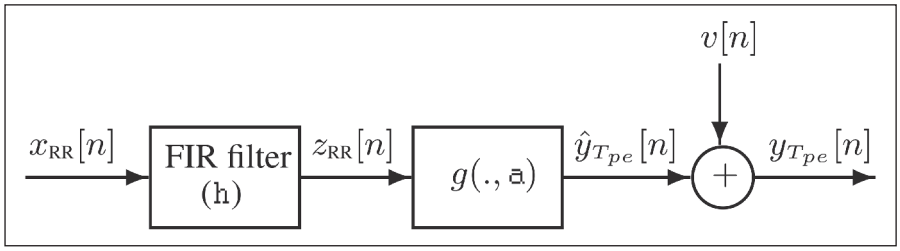

Figure 1 Block diagram describing the relationship between the T_{pe} interval and the RR interval, which consists of a time invariant FIR filter, with impulse response $\mathbf{h}$, and a nonlinear function described by vector a. v[n] accounts for the modeling error.

Table 1 Example of the derivatives of three regression functions $g_k(\mathbf{z}_{RR}, \mathbf{a})$, with respect to $\mathbf{z}_{RR}$ and $\mathbf{a}$. $\left(\frac{\partial g_k(\mathbf{z}_{RR},\mathbf{a})}{\partial \mathbf{z}_{RR}}\right)$ diag is the diagonal of the matrix $\frac{\partial g_k(\mathbf{z}_{RR},\mathbf{a})}{\partial \mathbf{z}_{RR}}$. $\mathbf{1}$ represents a N-length vector of ones. All mathematical expressions are element-wise.

Model g_k	diag $\left(\frac{\partial g_k(\mathbf{z}_{RR},\mathbf{a})}{\partial \mathbf{z}_{RR}}\right)$	$\frac{\partial g_k(\mathbf{z}_{RR},\mathbf{a})}{\partial a_0}$	$\frac{\partial g_k(\mathbf{z}_{RR},\mathbf{a})}{\partial a_1}$
$a_0 + a_1 \mathbf{z}_{RR}$	$a_1 1$	1	$\mathbf{z}_{RR}$
$a_0 + \frac{a_1}{\mathbf{z}_{RR}}$	$\frac{-a_1}{\mathbf{z}_{RR}^2}$	1	$\frac{1}{\mathbf{z}_{RR}}$
$a_0 \cdot \mathbf{z}_{RR}^{a_1}$	$a_0 a_1 \mathbf{z}_{RR}^{a_1-1}$	$\mathbf{z}_{RR}^{a_1}$	$a_0 \log(\mathbf{z}_{RR}) \mathbf{z}_{RR}^{a_1}$

$$\frac{\partial \tilde{J}}{\partial \tilde{\mathbf{h}}} = \frac{\partial \tilde{J}}{\partial g_k(\mathbf{z}_{RR}, \mathbf{a})} \frac{\partial g_k(\mathbf{z}_{RR},\mathbf{a})}{\partial \mathbf{h}} \frac{\partial \mathbf{h}}{\partial \tilde{\mathbf{h}}} + \beta^2 \frac{\partial \|\boldsymbol{D}\mathbf{h}\|^2}{\partial \mathbf{h}} \frac{\partial \mathbf{h}}{\partial \tilde{\mathbf{h}}}$$

Figure 2 Application of the chain rule to differentiate $\tilde{J}$ with respect to $\tilde{\mathbf{h}}$

$$\begin{pmatrix} dh[1] \\ \vdots \\ dh[N] \end{pmatrix} = \begin{bmatrix} \frac{\partial h[1]}{\partial \tilde{h}[1]} & \cdots & \frac{\partial h[1]}{\partial \tilde{h}[N]} \\ \vdots & \ddots & \vdots \\ \frac{\partial h[N]}{\partial \tilde{h}[1]} & \cdots & \frac{\partial h[N]}{\partial \tilde{h}[N]} \end{bmatrix} \begin{pmatrix} d\tilde{h}[1] \\ \vdots \\ d\tilde{h}[N] \end{pmatrix}$$

Figure 3 Jacobian matrix relates perturbations of $\tilde{\mathbf{h}}$ perturbations of $\mathbf{h}$

$$\frac{\partial \mathbf{h}}{\partial \tilde{\mathbf{h}}} = \begin{bmatrix} \frac{\partial h[1]}{\partial \tilde{h}[1]} & \cdots & \frac{\partial h[1]}{\partial \tilde{h}[N]} \\ \vdots & \ddots & \vdots \\ \frac{\partial h[N]}{\partial \tilde{h}[1]} & \cdots & \frac{\partial h[N]}{\partial \tilde{h}[N]} \end{bmatrix} = \begin{pmatrix} \frac{2\tilde{h}[1]\sum \tilde{h}[i]^2 - 2\tilde{h}[1]^3}{\left(\sum \tilde{h}[i]^2\right)^2} & \cdots & \frac{-2\tilde{h}[N]\tilde{h}[1]^2}{\left(\sum \tilde{h}[i]^2\right)^2} \\ \vdots & \ddots & \vdots \\ \frac{-2\tilde{h}[1]\tilde{h}[N]^2}{\left(\sum \tilde{h}[i]^2\right)^2} & \cdots & \frac{2\tilde{h}[N]\sum \tilde{h}[i]^2 - 2\tilde{h}[N]^3}{\left(\sum \tilde{h}[i]^2\right)^2} \end{pmatrix}$$

Figure 4 Explicit expression of the Jacobian matrix in terms of the components $\tilde{h}[i]$

$$\begin{aligned} \tilde{J}_k &= \| \boldsymbol{y}_{Tpe} - g_k(\mathbf{z}_{RR}, \mathbf{a}) \|^2 + \beta^2 \| \boldsymbol{D}\mathbf{h} \|^2 \\ &= \left(\boldsymbol{y}_{Tpe} - g_k(\mathbf{z}_{RR}, \mathbf{a}) \right)^T \left(\boldsymbol{y}_{Tpe} - g_k(\mathbf{z}_{RR}, \mathbf{a}) \right) + \beta^2 \| \boldsymbol{D}\mathbf{h} \|^2 \end{aligned}$$

Figure 5 Explicit expression of $\tilde{J}_k$

each regression function g_k. The estimated $\hat{\boldsymbol{y}}_{Tpe}$ can be expressed as $g_k(\mathbf{z}_{RR}, \mathbf{a})$, which depends on $\mathbf{h}$ by the relationship $\mathbf{z}_{RR} = \mathbf{x}_{RR} \cdot \mathbf{h}$. In order to differentiate $\tilde{J}_k$ with respect to the first variable vector $\tilde{\mathbf{h}}$ the chain rule was applied (▶Figure 2), where the first term corresponds to the estimation error and the second one to the regularization error.

In ▶Figure 2 the derivative $\frac{\partial \mathbf{h}}{\partial \tilde{\mathbf{h}}}$, also called Jacobian matrix, is defined as the matrix of the derivatives of a vector-valued function with respect to another vector. It represents the effect on $\mathbf{h}$ of a perturbation $\partial\tilde{\mathbf{h}}$ of the vector $\tilde{\mathbf{h}}$: (▶Figure 3), Therefore, the derivative $\frac{\partial \mathbf{h}}{\partial \tilde{\mathbf{h}}}$ was computed as can be seen in ▶Figure 4). Also in ▶Figure 2 there is the factor $\frac{\partial \tilde{J}}{\partial g_k(\mathbf{z}_{RR},\mathbf{a})}$.

To compute it, first note that $\tilde{J}_k$ can be expressed as in ▶Figure 5. Therefore,

$$\frac{\partial \tilde{J}_k}{\partial g_k(\mathbf{z}_{RR},\mathbf{a})} = -2\left(\boldsymbol{y}_{Tpe} - g_k(\mathbf{z}_{RR},\mathbf{a})\right)^T \quad (7)$$

Another factor in ▶Figure 2 is $\frac{g_k(.,\mathbf{a})}{\partial \mathbf{h}}$. Taking into account that g_k depends on $\mathbf{z}_{RR}$, and $\mathbf{z}_{RR} = \boldsymbol{X}_{RR}\mathbf{h}$:

$$\frac{\partial g_k(\mathbf{z}_{RR},\mathbf{a})}{\partial \mathbf{h}} = \frac{\partial g_k(\mathbf{z}_{RR},\mathbf{a})}{\partial \mathbf{z}_{RR}} \frac{\partial \mathbf{z}_{RR}}{\partial \mathbf{h}} = \frac{\partial g_k(\mathbf{z}_{RR},\mathbf{a})}{\partial \mathbf{z}_{RR}} \boldsymbol{X}_{RR} \quad (8)$$

$\frac{\partial g_k(\mathbf{z}_{RR},\mathbf{a})}{\partial \mathbf{z}_{RR}}$ is a matrix since $\partial g_k(\mathbf{z}_{RR}, \mathbf{a})$ and $\partial \mathbf{z}_{RR}$ are vectors. Besides, a perturbation of the i-th element of the vector $\mathbf{z}_{RR}$ produces an effect only on the i-th element of the vector $g_k(\mathbf{z}_{RR}, \mathbf{a})$, and then $\frac{\partial g_k(\mathbf{z}_{RR},\mathbf{a})}{\partial \mathbf{z}_{RR}}$ is a diagonal matrix.

For the three regression model examples shown in ▶Equations 2–4, the diagonals of are shown in ▶Table 1.

Finally, the derivative $\frac{\partial \|\boldsymbol{D}\mathbf{h}\|^2}{\partial \mathbf{h}}$ in ▶Figure 2 can be calculated as:

$$\frac{\partial \|\boldsymbol{D}\mathbf{h}\|^2}{\partial \mathbf{h}} = \frac{\partial}{\partial \mathbf{h}} (\boldsymbol{D}\mathbf{h})^T (\boldsymbol{D}\mathbf{h}) \quad (9)$$
$$= 2(\boldsymbol{D}\mathbf{h})^T \boldsymbol{D}$$

Eventually, $\frac{\partial \tilde{J}}{\partial \tilde{\mathbf{h}}}$ was computed by introducing ▶Equations 7–9 into ▶Figure 2.

In order to differentiate the cost function $\tilde{J}$ with respect to the second variable vector **a**, the chain rule was also applied:

$$\frac{\partial \tilde{J}}{\partial \mathbf{a}} = \frac{\partial \tilde{J}}{g_k(\mathbf{z}_{RR}, \mathbf{a})} \frac{g_k(\mathbf{z}_{RR}, \mathbf{a})}{\partial \mathbf{a}}$$

The first term in the above expression was already calculated in ▶Equation 7, while the second term is a Nx2 matrix where the first column corresponds to $\frac{g_k(\mathbf{z}_{RR}, \mathbf{a})}{\partial a_0}$ and the second column to $\frac{g_k(\mathbf{z}_{RR}, \mathbf{a})}{\partial a_1}$, both shown in ▶Table 1.

2.3. Optimization Technique

In this work, a quasi-Newton optimization technique, the BFGS (Broyden-Fletcher-Goldfarb-Shanno), was used to minimize the cost function $\tilde{J}_k(\tilde{\mathbf{h}}, \mathbf{a})$ [8]. BFGS quasi-Newton method estimates the Hessian (or the Hessian inverse) matrix preserving symmetry and positive definiteness. In each step, the estimation of the Hessian matrix is updated using the gradient information [8]. In order to compute the step size along each descent direction, obtained by the quasi-Newton method, a parabolic and a golden ratio line searches were used [9].

2.4 Study Population and Characterization of Repolarization Adaptation

ECG recordings of fifteen volunteers sampled at 1000 Hz were obtained during a head-up tilt test trial and used to characterize T_{pe} and QT rate adaptation. The tilt test protocol generated two step-like RR changes with stabilized RR intervals after each of them (▶Figure 6, top panel).

ECG delineation was performed using a wavelet-based delineator [10]. RR, QT and T_{pe} intervals were computed from the ECG delineation marks in leads V2 and V4.

The time required for T_{pe} and QT to complete 90% of their rate adaptation, denoted by t_{90}, was computed by setting a threshold of 0.1 to the cumulative sum of the filter impulse response:

$$t_{90} = \frac{1}{f_s} \arg\max_n \left(\sum_{i=n}^{N} h[i] > 0.1 \right).$$

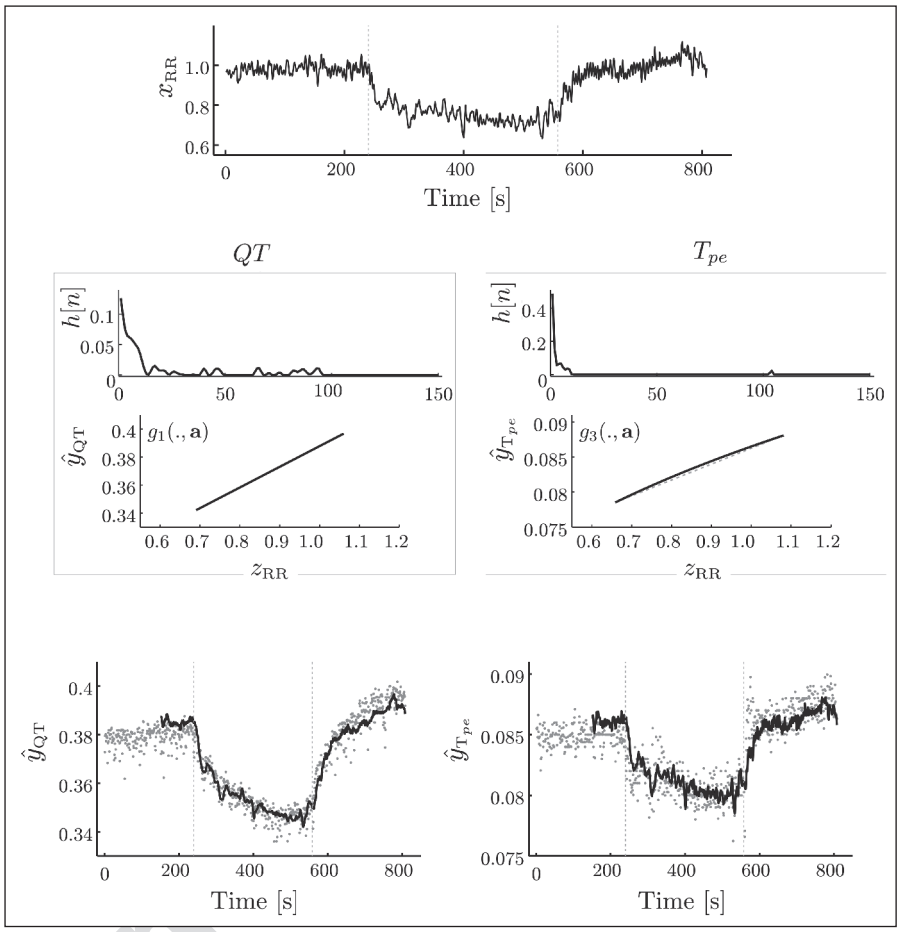

Figure 6 Top panel: $\mathbf{x}_{RR}$ series obtained from a subject of the study population. Middle and bottom panels: on the left, an example of how the reconstruction $\hat{y}_{QT}$ (black solid line) of the QT interval series y_{QT} (gray dots), is obtained by x_{RR} through the estimations of **h** and $g_k(.,\mathbf{a})$. In this example, the optimum regression model for the QT interval is the linear one ($k = 1$). On the right, analogously for the T_{pe}, the reconstruction $\hat{y}_{Tpe}$ (black solid line) is shown. The optimum model regression in this case is the parabolic function ($k = 3$). In dashed gray line, the linear function is also depicted for comparison purposes.

3. Results and Discussion

An example of the reconstruction of the $y_{QT}[n]$ and $y_{Tpe}[n]$ series, after estimating the corresponding h[n], the regression model k and the coefficient vector **a** are shown in ▶Figure 6. The reconstructed $\hat{y}_{Tpe}[n]$ and $\hat{y}_{QT}[n]$, shown in black solid lines, begin after 150 seconds corresponding to the length of the filter h[n]. The estimated regression functions in this example are different for the QT (linear model) and for the T_{pe} series (parabolic model).

In ▶Figure 7, the median, first and third quartile of the T_{pe} rate adaptation, $\sum_{i=n}^{N} h[i]$, across the 15 recordings are shown

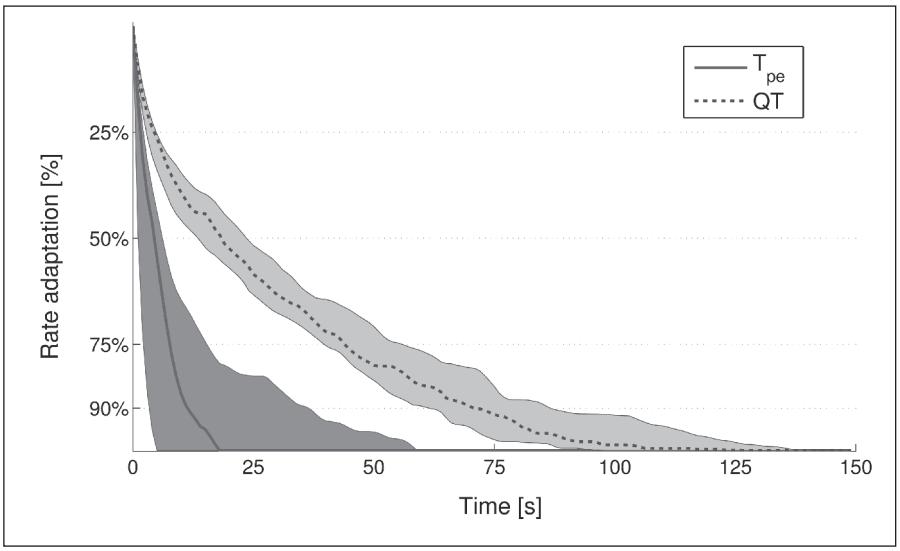

Figure 7 Median, first and third quartile of the rate adaptation $\sum_{i=n}^{N} h[i]$, of T_{pe} and QT intervals.

and compared to those of the QT interval. t_{90} values are 23 s, in mean, for T_{pe} to complete 90% of the rate adaptation and 74 s for QT which is within clinical ranges [5]. The characterization of T_{pe} rate adaptation shows that T_{pe} is rate related and it has a shorter memory lag than the QT interval.

The cost function from ▶Equation 6 with the constraints $\sum_{i=1}^{N} h[i] = 1 = 1$ and $h[i] \geq 0$, is a convex function in a convex domain. Therefore, the problem has a unique solution. When comparing the proposed methodology with the one used in [5], which solved the model using a derivative free optimizer such as DiRect method, we obtained a ten times faster convergence for the present method (obtaining the same results within the floating point precision). The algorithm proposed is faster since the restrictions are included in the cost function, resulting in an unconstrained optimization problem. Furthermore, the gradient was computed explicitly.

4. Conclusions

In this work an estimation strategy for the parameters of a model aimed at characterizing rate adaptation of repolarization features has been proposed. Physiological restrictions have been included into the cost function, which allowed the use of descent unconstrained optimization methods with a fast convergence and efficiency. The evaluation of the method on a tilt test database shows results on rate adaptation times that are within clinical ranges.

References

1. Antzelevitch C, Viskin S, Shimizu W, Yan G-X, Kowey P, Zhang L, et al. Does Tpeak-Tend Provide an Index of Transmural Dispersion of Repolarization? Heart Rhythm Off J Heart Rhythm Soc 2007; 4 (8): 1114–1119.
2. Andersen MP, Xue JQ, Graff C, Kanters JK, Toft E, Struijk JJ. New descriptors of T-wave morphology are independent of heart rate. J Electrocardiol 2008; 41 (6): 557–561.
3. Smetana P, Batchvarov V, Hnatkova K, John Camm A, Malik M. Sex differences in the rate dependence of the T wave descending limb. Cardiovasc Res 2003; 58 (3): 549–554.
4. Mincholé A, Pueyo E, Rodríguez JF, Zacur E, Doblaré M, Laguna P. Quantification of restitution dispersion from the dynamic changes of the T-wave peak to end, measured at the surface ECG. IEEE Trans Biomed Eng 2011; 58 (5): 1172–1182.
5. Pueyo E, Smetana P, Caminal P, de Luna AB, Malik M, Laguna P. Characterization of QT interval adaptation to RR interval changes and its use as a risk-stratifier of arrhythmic mortality in amiodarone-treated survivors of acute myocardial infarction. IEEE Trans Biomed Eng 2004; 51 (9): 1511–1520.
6. Hansen PC. Rank-Deficient and Discrete Ill-Posed Problems: Numerical Aspects of Linear Inversion. Society for Industrial and Applied Mathematics; p 268.
7. Hansen P. Analysis of Discrete Ill-Posed Problems by Means of the L-Curve. Siam Rev 1992; 34 (4): 561–580.
8. Nocedal J, Wright SJ. Numerical Optimization. Springer; 2000. pp 135–143.
9. Press WH, Teukolsky SA, Vetterling WT, Flannery BP. Numerical Recipes Art Scientific Computing 3rd Edition | Numerical recipes | Cambridge University Press. 2007.
10. Martínez JP, Almeida R, Olmos S, Rocha AP, Laguna P. A wavelet-based ECG delineator: evaluation on standard databases. IEEE Trans Biomed Eng 2004; 51 (4): 570–581.